

CRL: Class Representative Learning for Image Classification

Mayanka Chandrashekar, *Member, IEEE*, and Yugyung Lee, *Member, IEEE*

Abstract—Building robust and real-time classifiers with diverse datasets are one of the most significant challenges to deep learning researchers. It is because there is a considerable gap between a model built with training (seen) data and real (unseen) data in applications. Recent works including Zero-Shot Learning (ZSL), have attempted to deal with this problem of overcoming the apparent gap through transfer learning. In this paper, we propose a novel model, called Class Representative Learning Model (CRL), that can be especially effective in image classification influenced by ZSL. In the CRL model, first, the learning step is to build class representatives to represent classes in datasets by aggregating prominent features extracted from a Convolutional Neural Network (CNN). Second, the inferencing step in CRL is to match between the class representatives and new data. The proposed CRL model demonstrated superior performance compared to the current state-of-the-art research in ZSL and mobile deep learning. The proposed CRL model has been implemented and evaluated in a parallel environment, using Apache Spark, for both distributed learning and recognition. An extensive experimental study on the benchmark datasets, ImageNet-1K, CalTech-101, CalTech-256, CIFAR-100, shows that CRL can build a class distribution model with drastic improvement in learning and recognition performance without sacrificing accuracy compared to the state-of-the-art performances in image classification.

I. INTRODUCTION

Recent advances in deep learning (DL) have improved the state-of-the-art researches in the data-driven approaches and applications in a wide range of domains. However, building robust and real-time classifiers with diverse datasets is one of the most significant challenges to deep learning researchers. It is because there is a considerable gap between a model built with training (seen) data and real (unseen) data in applications [5], [28], [61]. The current deep learning research assumes strong boundaries between data, between data and models, and between models in deep learning. The new paradigm focuses on the universal representation of diverse datasets.

There has been increasing attention on Zero-Shot Learning (ZSL) [61] and one-shot/few-shot learning (FSL) [27], [58]. These efforts aim to build the ability to learn from a few examples or even without seeing them. Alternatively, it is required to represent and match new instances on a semantic space, which results in minimizing training efforts and maximizing learning outcomes. They focus on active transfer learning by fully leveraging information from pre-trained models. The seamless integration of unlabeled data from the seen/unseen classes is possible through the expressive representations of multi-model embeddings, including semantic, word, visual

embeddings. However, there are the notable limitations of the ZSL or FSL approaches: Many of them are relying on semantic embeddings in a common semantic space having a generative model [9], [23], [42].

The recent ZSL works demonstrated their effectiveness in transferred from prior experiences to new classes, which is a form of transfer learning. The most used semantic space in the ZSL model is supported by a joint embedding framework called Label-Embedding Space [61], [66] containing a combination of visual embeddings and word embeddings; or Engineering Semantic Space called Attribute Space, which uses attribute annotations for the ZSL model [1]. In contrast to prior work, we mainly extract the deep neural network features learned from visual inputs of seen classes creating image representatives, and we do not rely on any other features such as attribute annotations or word embeddings.

Similar to our approach in the feature extraction, there are active efforts [30], [71] for extracting important features from Convolutional Neural Networks (CNNs) such as Inception or ResNet. Mahendran et al. [30] analyzed the preserved deep features through inverting the fully-connected layers. Zhou et al. [71] built the class activation map using CNN features for the localization of the objects in the images for the discriminative image regions. Unlike [30] and [71], we are interested in generating class representatives using CNN features.

The goal is to propose an innovative model called *Class Representative Learning (CRL)* for image classification for seen and unseen data. In this model, the focus is on creating a universal representation called the class representatives using the source environment, which is typically pre-trained deep learning models. Given this goal, architectural improvements are not our purpose; instead, we explore universal representatives that could be used for classification. It is desired to enable the universal representation to be trained from any existing architectures or datasets with reduced efforts and resources. The minimum requirement for the CRL model is to have a suitable *source* (pre-trained) CNN model that can be mapped to the given datasets (*target*).

The CRL model can be classified as transfer learning, called meta-learning [39], [67]. The basic idea behind transfer learning is to use previously learned knowledge on different domains or tasks. The CRL model is based on the transductive approach that aims to project the target data onto a source environment for the extraction of features by mapping to unify the input spaces. The transductive property in transfer learning is to derive the values of the unknown function for points of interest (class-based or instance-based) from the given data

M.Chandrashekar (mckw9@mail.umkc.edu) and Y. Lee (leeyu@umkc.edu) are with the Department of Computer Science and Electrical Engineering, University of Missouri, Kansas City, MO, 64110 USA

(source environment or source domain) [57], [61].

The CRL model poses the property of being selective during inferencing. In other words, the CRL model can classify an input image to either source labels or target labels or both. Due to this property, the CRL model can behave like a traditional classification model. The Convolution Neural Network-based Classification models tend to be high in parameter requirements to achieve state-of-the-art accuracy [7], [54]. To show the superiority of the CRL model developed in this study, we have compared our CRL model against other state-of-the-art deep learning models.

The contributions of this paper can be summarized as follows:

- The proposed model (CRL) is an efficient way of building class-level classifiers by utilizing features from a pre-trained model in Convolutional Neural Network for classification problems.
- The CRL has the ability to build models for the similarity distribution of CRs for given datasets and estimate the CR accuracies in the classification.
- A comprehensive evaluation of the proposed model has been conducted with deep learning models, Zero-Shot Learning (ZSL) using the four benchmark datasets in terms of time and accuracy. In addition, CRL was compared with the MobileNet models [45], [45], [73].

II. RELATED WORK

A. Transfer Learning

Recent studies have indicated the importance of transfer learning (TL) [26], [56] that aims to maximize the learning outcome by transferring a model developed for a task for building a model on another task. NASNet [73] explored the possibility of transferring from what learned from a small dataset (e.g., CIFAR-10) to a larger dataset (ImageNet-1K) through searching and utilizing a core architectural building block from the small dataset.

He et al. [18] have shown that pre-trained models with an extensive data set like ImageNet-1K or with a small dataset like a subset of MS COCO have incredible influence in computer vision. Initialization with pre-trained models or evaluating with pre-trained features (e.g., unsupervised learning [36]) can reduce efforts and produce better results in Deep Learning (DL). It is possible because pre-training models are widely available, and learning from the models is faster than building from scratch.

The DL community has extensively studied transfer Learning [26], [56]. The transfer learning from ImageNet-1K in Decaf [10] showed substantial improvements compared to learning from image features. Ravi et al. [39] also presented a meta-learner model that supported the quick convergence of training with a new task using few-shot learning.

Pan et al. [35] defined an inductive transfer learning as cross-domain learning where the target task is different from the source task. The data in the target domain are required to induce a predictive model that can be transferred from the source domain to the target domain. Our model is similar to the Feature-representation-transfer defined by Pan et al.

However, the difference is that our model was encoded based on the aggregation of the high-level features extracted from Convolutional Neural Networks.

In our paper, we used a pre-trained model only for feature extraction, but training is not required with new data. After the fully connected layers are removed from the entire network, the rest will be mainly used for feature extraction for new data. Thus, the use of the pre-trained model in our study is different from others since we only use it as a reference model for extracting features for new data.

B. Universal Representation

Ubernet [25] is a *universal* CNN that allows solving multiple tasks in a unified architecture efficiently. It is through the end-to-end network training with a single training set for diverse datasets and low memory complexity. Universal representations [6], [40] perform well for visual domains in a uniform manner and have proven to be efficient for multiple domain learning in relatively small neural networks.

Rebuff et al. [41] demonstrated that universal parametric families of networks could share parameters among multiple domains using parallel residual adapter modules. Similar to our work, all these works presented universal representations for multiple domains or multiple tasks. However, unlike CRL, none of them focus on dynamically generating a model for multiple domains.

In this paper, we define *Source Environment* for providing a basis for feature selection as well as a uniform representation of a set of heterogeneous data sources for effective deep learning. Feature selection is a crucial step in machine learning since it directly influences the performance of machine learning. (e.g., as the right choice of features drives the classifier to perform well). However, Kapoor et al. [22] observed that finding useful features for multi-class classification is not trivial due to the volume in the high-dimensional feature space as well as the sparseness over the search space.

Dictionary learning [47] was presented to determine the subspaces and build dictionaries by efficiently reducing dimensionality for efficient representations of classes of images. The critical contribution of the work is the reduction of sparsity constraints and the improvement of accuracy by identification of the most essential components of the observed data.

From the extracted set of relevant features from images and quantizing them with these bags of visual words, we will further build up a visual CR vector for each class by combining these primitive features. The visual CRs will be used for efficient learning as well as recognition with large scale multi-class datasets.

C. Lightweight Deep Learning

Recently, there has been an increasing demand for mobile applications for small networks or dynamic networks in deep learning. There have been several deep neural architectures to strike an optimal balance between accuracy and performance. The lightweight deep learning was achieved using three types of layer compression techniques namely: weight compression, Convolution compression and adding a single layer [32].

Weight compression is the primitive technique used to create a lightweight model. MobileNet-V1 [20] and Shufflenet [70] used a convolution compression technique in its architecture, specifically depth-wise separable convolutions and point-wise group convolution, respectively.

As an extension of the previous works, MobileNet-v2 [45] added a new layer, namely an inverted residual layer, with a narrow bottleneck to create a lightweight model. In NasNet Mobile [73], a new paradigm, called Neural Architecture Search (NAS), was proposed with reinforcement learning for knowledge transfer. In general, architectural changes are typically considered to achieve a lightweight model. In the CRL model, we have obtained a lightweight model through the flexibility of representation concerning the class.

D. Matching Networks

Few-shot classification [27], [58] is to label new classes which are not seen in training, but through matching with only a few examples of each of these classes. The matching networks are similar to a weighted nearest-neighbor classifier in an embedding space. The embedding in the matching networks was built as a form of sampled mini-batches, called episodes, during training. Notably, matching networks [58] is similar to our work in terms of mapping an attention-based embedding to a query set for predicting classes. However, our model is different from these works since we can build a dynamic model for multiple classes by assembling a set of a single class classifier, called Class Representative, built one by one independently.

A meta-learning approach [39] aims to build a custom model for each episode based on Long Short-Term Memory (LSTM), unlike others building each episode over multiple episodes. The prototypical networks [50] built a class prototype by computing the mean of the training set in the embedding space and find the nearest class prototype for a query set as inferencing. This approach is very similar to our work in terms of building the class's prototype as an abstraction of the class by learning an embedding of the meta-data into a shared space. Recently, Wang et al. [62] extended the performance of Zero-Shot Learning and Few-Shot Learning using latent-space distributions of discriminative feature representations. Similar to our approach, they used only the feature extractor of the CNN model. However, they are different from our work in terms of the following aspects: (1) they used variational autoencoder (VAE) while we are using a vector space model with a cosine similarity measurement, (2) they built a model for all classes in any given dataset while we are building a model class by class. They focused on learning an embedding of the meta-data into a shared space. However, in our work, we build CRs class by class. Thus, once the CR is generated, there is no dependence between CRs. Due to the independence between CRs, we can build multi-class models dynamically.

E. Zero-Shot Learning

Zero-Shot Learning (ZSL) defined a semantic encoding for predicting new classes by using a standard feature set derived from a semantic knowledge base [34]. All well-known

works have worked on learning and understanding explicit and external attributes. Much of the early work adapted from the original definition of the semantic knowledge base in Zero-Shot Learning [34], focused on attributes solely based on visual feature learning. Some of the works in the feature learning include boosting techniques [63], object detection [55], chopping algorithm [12], feature adaption [4], and linear classifiers [3].

The recent works of Zero-Shot Learning can be categorized into Engineered Semantic Spaces (ESS) and Learned Semantic Spaces (LSS) according to the semantic space type and ZSL methods in Wang et al. [61]. ESS can be further sub-categorized into Attribute Space, Lexical Space, and Text-Keyword Space; and LSS into Label-Embedding Space, Text-Embedding Space, and Image-Representation Space. The Zero-Shot Learning method is classified into Classifier-based Methods and Instance-Based Methods. According to this categorization, the CRL model can be classified as Image Representation Semantic Space and Instance-Based Method, specifically Projection Method (see Figure 1). The Projection method provides insights for labeled instances from an unseen class by projecting both the instance's feature space and the semantic space prototype to a shared space [61].

Table I shows existing Zero-Shot Learning (ZSL) models that were compared with our model in the evaluation section. Most of the recent work includes two kinds of semantic spaces, namely Label-Embedding Spaces [61], [66] and Attribute Spaces [61] (also known as Probability Prediction Strategy [66]). Label-Embedding Spaces focuses on learning a projection strategy that connects image semantic features to labels, in which labels are represented a high dimensional embedding using Word2Vec [31] or Glove [37]. Image Features in Label-Embedding Spaces are typically learned from Convolutional Neural Networks [?], [1], [14], [17], [43], [64]. Attribution Spaces or Probability Prediction initially focuses on pre-training attribute classifiers based on source data [66], where an attribute is defined as a list of terms describing various properties of given a class [61]. Each attribute forms the dimensions of class; value is typically given if a class contains the attribute or not [29], [33], [67].

Pure Image Representation Space-based ZSL is rarely observed, one of the very first works was to use Image Deep Representation and Fisher Vector for the ZSL Project method [60] and an extension of this approach was used to create unsupervised domain adaptation [59]. Zhu et al. used the partial image representation method to achieve a universal representation for action recognition [72].

III. CLASS REPRESENTATIVE LEARNING MODEL

The significance of the Class Representative Learning (CRL) model is its competence to project the input data to a global space that is specified by the activation of neurons in the pre-trained model such as CNN. The space of the CRL model is similar to the universal representation proposed by Tamaazousti et al. [53], where visual elements in the configuration (e.g., scale, context) can be encoded universally for transfer learning. The fundamental concept of the CRL

Table I: Related Work: Zero-Shot Learning Methods

Approach	Semantic Space	Zero-Shot Learning Method
CRL Model (ours)	LSS - Image Representation Space	Instance-Based (Projection Method)
Deep-WMM-Voc [16]	LSS - Label Embedding Space	Classifier-Based
SAE [24]	ESS- Attribute Space & LSS-Label Embedding Space	Classifier-Based
ESZSL [43]	ESS- Attribute Space	Classifier-Based
Deep-SVR [29] [11]	ESS - Attribute Space	Classifier-Based
Embed [69]	LSS - Label Embedding Space	Instance-Based
ConSE [33]	LSS - Label Embedding Space	Instance-Based
DeViSE [14]	LSS - Label Embedding Space	Classifier-Based
AMP [17]	LSS - Label Embedding Space	Classifier-Based

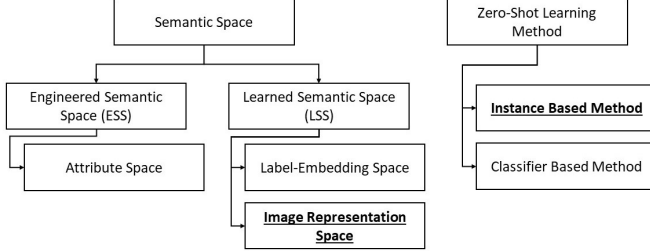


Figure 1: Types of Semantic Space and ZSL Methods

* The CRL model belongs to the highlighted types.

model is its ability to create the representatives of class in parallel and independently without depending on other classes.

As shown in Figure 2, the CRL model is composed of two primary components such as CR Generation and CR-based Inferencing. The model used to evaluate the CRL model is the Inception-V3 model that was pre-trained with ImageNet-1K [44]. The pre-trained model is the *Source* environment for the CRL model where no learning is happening, but the *Source* environment was mainly used as a reference standard for producing a feature vector of the input data in space. Figure 2(a) shows the *Source* environment (i.e., Pre-trained model), and Figure 2(b) shows the inferencing process with CRs on how a new image is projected on the *Source* environment and is mapped it on to the CRs for classification.

A. Problem Setup

Assume the given source data $D_s = \{x_n, y_n\}_{n=1}^{m_s}$ of m labeled points with a label from the source class $1, \dots, S$, where $x_n \in \mathbb{R}$ is the feature of the n^{th} image in the source data and $y_n \in \mathbb{S}$ where $\mathbb{S} = \{1, \dots, C_s\}$ is the set of source classes. The target data is represented as $D_t = \{x_n, y_n\}_{n=1}^{m_t}$ classes where $y_n \in \mathbb{T}$. The target classes \mathbb{T} are represented as $\{C_s + 1, C_s + 2, \dots, C_t\}$ where C total set of classes is $C = \mathbb{S} \cup \mathbb{T}$, where the total number of classes is $C_s + C_t$. For each class $c \in \mathbb{S} \cup \mathbb{T}$, has a Class Representative $CR(c)$ which is the semantic representative of class c . Furthermore, the source label \mathbb{S} and the target label \mathbb{T} are considered such that $\mathbb{S} \cap \mathbb{T} = \emptyset$. For simplicity, the source and target datasets have overlapped labels but these overlapped classes are considered distinct. In the CRL model, the source data are considered as *seen*, and the target data are *unseen*. In other words, the target data are not used in the learning process. Table II summarizes all the symbols and notations used in the CRL model.

Table II: Formal Symbol and Notations in the CRL model

Notation	Description
$D_s \& D_t$	Source and Target Domain
$m_s \& m_t$	#Data Points from Source and Target, respectively
$C_s \& C_t$	#Classes from Source and Target, respectively
$\mathbb{S} \& \mathbb{T}$	Source and Target Label Set
C	#Classes
x	Feature Vector of Labeled Data Point
y	Label of Data Point
j	#Neurons in a Given Activation Layer
AFM_s	Activation Feature Map $\{b_1, b_2, \dots, b_j\}$
$CR(c)$	Class Representative of Class c where $c \in C$
$CR(c)$	Class Representative Set $\{CR_c^1, CR_c^2, \dots, CR_c^n\}$
x^*	Unlabeled Data Point
CRC	Class Representative Classifier
$CRFS^n$	Class Representative Feature Space
n	Dimensions of the $CRFS$

The goal of the CRL model is that given a new test data x^* , the model will classify it into one of the classes y^* where $y^* \in C$. The CRL model defines a universal problem for a classification approach as well as a traditional ZSL approach as follows:

- Classification (CL) Approach: $y^* \in \mathbb{S}$
- Zero-Shot Learning (ZSL) Approach: $y^* \in \mathbb{S} \cup \mathbb{T}$

In both models, there are no dependencies among CRs. The difference between these two models is in the properties of the inference. If the CR of the target set was introduced, then it would be *CL*, and if both CRs of the source set and the target set are introduced, then it would be *ZSL*.

B. CR Definition and Property

Definition 1: Activation Feature Map

Activation Feature Map (AFM) is a vector of features extracted from a base model that will be defined by a pre-trained model for any given instance. For a given input, AFM represents the features that are defined by the activation of neurons in the base model. The AFM dimensionality is the number of neurons in the selected layer of the base model. In other words, it is the number of distinct neuron activating neurons occurring in the corpus. The n dimensional AFM forms the basis for the Semantic Space that is defined in Zero-Shot Learning (ZSL).

Definition 2: Class Representative

Class Representative (CR) is a representative of K instances in a single class. The Activation Feature Map of the CR is a unique characteristic pattern of visual expression that occurs as

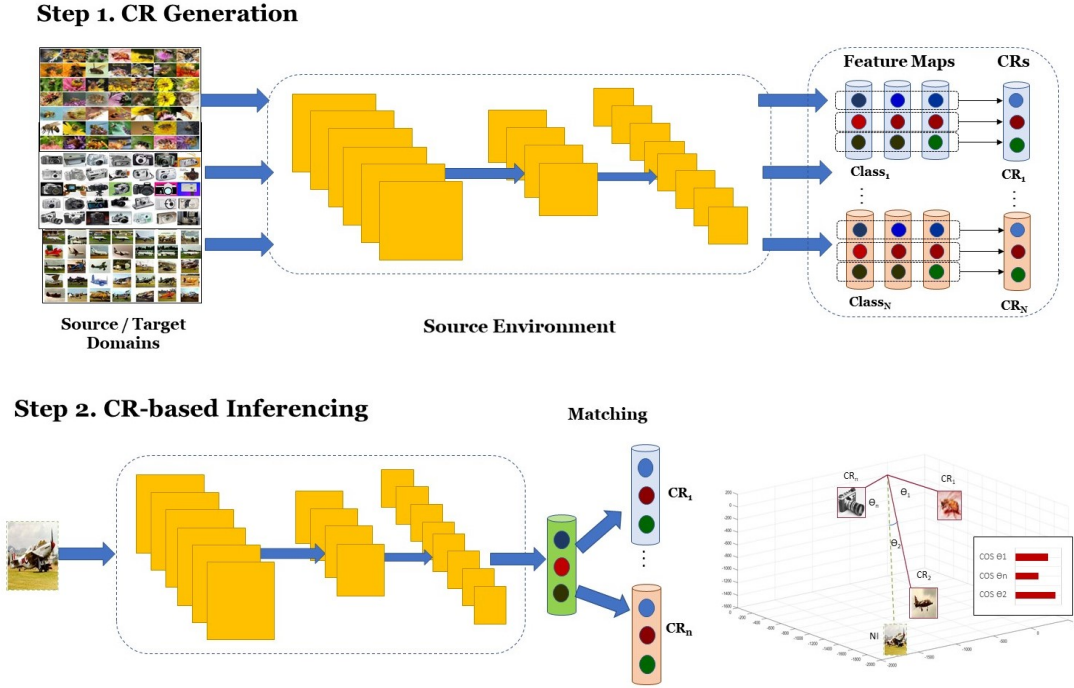


Figure 2: Class Representative Learning (CRL) Architecture

a result of the deep learning process in Convolutional Neural Networks (CNN). Thus, CR is an abstraction of instances of a class by computing an aggregation of the average mean vectors of the AFM for the K instances. The CR characterizes a class and differentiates one class against another.

The Class Representatives $CR(c)$ for Class c is represented as $\{CR_c^1, CR_c^2, \dots, CR_c^n\}$ with n dimensions. Each dimension corresponds to a separate feature. If a feature occurs in CR, its value in the vector is non-zero.

Definition 3: Class Representative Classifier

A Class Representative Classifier $CRC : I^d \rightarrow C$ maps an input image space I^d of the dimension d to the Class Representative Feature Space $CRFS^n$ of the dimension n to classify it to Class C . (CRFS is defined in Definition 4). CRC is defined as a composition of two functions as shown in Equation 1.

$$\begin{aligned} CRC &= L(S(\cdot)) \\ S : I^d &\rightarrow CRFS^n \\ L : CRFS^n &\rightarrow C \end{aligned} \quad (1)$$

The CRC model first maps the Input Space I^d to Class Representative Feature Space $CRFS^n$ with n dimensions. $CRFS^n$ further maps into Class C . The mapping function S represents the source environment, which aids the transformation of the input data into the Feature Space. (The source environment is further discussed in Section III-B). For example, the input of a *dog* image with dimensions [299x299x3] is mapped into Class Representative Space (as defined in Definition 4). Then, the CRFS will be labelled with the class *dog* through the classification process [15], [16], [34].

Definition 4: Class Representative Feature Space

Class Representative Feature Space (CRFS) is a n dimensional semantic feature map in which each of the n dimensions represents the value of a semantic property. These properties may be categorical and contain real-valued data or models from deep learning methods [34]. The Class Representative Feature Space represents n dimensional representative features as a form of the Activation Feature Map (AFM).

The design of the CRFS is based on the equations defines in [38]. The data points from $D_t \{(x^{(1)}, y^{(1)}), \dots, (x^{(m_t)}, y^{(m_t)})\}$ with each $x^{(i)} \in \mathbb{R}$ and $y^{(i)} \in \mathbb{T}$ (as shown in Equation 3. A set of the mean of the base features is defined as $x^{(i)}$. Note that the data points can also be defined in D_s , that will be used in CRFS to understand both source and target domains (refer to Section III-D).

$$\begin{aligned} D_t &= \{x^{(i)}, y^{(i)}\}_{i=1}^{m_t} \\ \hat{a}(x^{(i)}) &= \operatorname{argmin}_{a^{(i)}} \|x^{(i)} - \sum_j a_j^{(i)} b_j\|_2^2 + \beta \|a^{(i)}\|_1 \end{aligned} \quad (2)$$

$$\hat{D}_t = \{(\hat{a}(x^{(i)}), y^{(i)})\}_{i=1}^{m_t} \quad (3)$$

CRFS is created based on the base vectors $b = \{b_1, b_2, \dots, b_s\}$ with each $b_j \in R_n$. The base vector b is generated in the source environment using D_s . The activation $a = \{a^{(1)}, \dots, a^{(k)}\}$ with each $a^{(i)} \in R_s$ forms the semantic property of CRFS. Each dimension of an activation vector $a_j^{(i)}$ is the transformation of input $x_u^{(i)}$ using the base b_j . The number of bases s can be much larger than the input dimension n . The transformed target data points \hat{D}_t will be input for the Class Representative Generation.

Since each pair of $(x^{(i)}, y^{(i)})$ is independent of each other, our algorithm was designed with the CRCW (Concurrent Read

Concurrent Write) model which allows parallel computing, including I/O, with the shared memory and processors. The CRL's operation time is proportional to the number of the selected CRs across all processors. The CR Generation will be proportional to the input set per CR independent of the number of classes in a given dataset. The CR-based inferencing will be proportional to the number of CRs in a given model.

C. CR Generation

Class Representatives (CR) are generated using the nearest prototype strategy by aggregating feature vectors. The nearest mean feature vector with instances of the given class, i.e., Class Representatives, is computed for each class. Specifically, the average feature mean operation was used to summarize the instances of classes. For each class, the instances of each feature in the feature maps (e.g., 12K for a CNN layer) are aggregated into a simple mean feature in order to create its CR. The CR is an aggregated vector of the mean features for all the features in the feature maps.

For the Class Representative Generation, we considered the transformed Target Dataset \hat{D}_t as the input (as shown in Equation 2). As we emphasis on the parallelism and independence, we considered the individual activation vector $\hat{a}(x^{(i)})$ such that $y^i = c$, that will be used in formulating the CR as shown in Equation 4.

$$\begin{aligned} CR(c) &= \{CR^1, CR^2, \dots, CR^n\} \\ CR^j &= \frac{1}{N_c} \sum_{i=1}^{N_c} \hat{a}(x^{(i)}) \end{aligned} \quad (4)$$

where j ranges from 1 to n representing the feature dimensions, c is the class of the input image, and N_c is the number of data points for the class c . Class Representative of the given class c is represented as the group of CR features values CR^j where j ranges from 1 to n feature dimensions. CR^j is generated from the mean of AFM (refer to Equation 2) of every input image in a given class c as shown in Equation 4. The CR Generation can be conducted in parallel so that each CR of class independently can be generated. The parallel algorithm with CRCW (as explained in Section III-B) was implemented with Spark's broadcast variables for the CR Generation.

D. CR Feature Space: Source and Target Mapping

The Class Representative (CR) mapping is a variation of Multi-Discriminative Problem network [53]. This method is attempting to universalize a method that combines different but complementary features learned on different problems. The source domain problem is defined as the DP^s in the class when the Convolution Neural Network assigns to the input image the label corresponding to the classes provided by the source domain D . Similar to what is described in Pan et al. [35], we define our source and target domain based two aspects, namely Class Representative Feature Space (CRFS) and Marginal Distribution.

$$\begin{aligned} D_s &= CRFS_s, P(CR_s) \\ D_t &= CRFS_t, P(CR_t) \end{aligned} \quad (5)$$

As shown in Equation 5, the CR source domain D_s is a two-element tuple consisting of Source CR Feature Space $CRFS_s$ and Probability Distribution Function of CR $P(CR_s)$, where CR_s is Class Representatives from the source domain. The CR target domain D_t is also defined as a two-element tuple consisting of Target CR Feature Space $CRFS_t$ and Probability Distribution Function of CR, $P(CR_t)$, where CR_t Class Representatives were generated from the target domain.

$$\begin{aligned} D^* &= \max_x |P(CR_s) - P(CR_t)| \\ &P(CR_s) \forall CR_s \in CRFS_s \\ &P(CR_t) \forall CR_t \in CRFS_t \end{aligned} \quad (6)$$

As shown in Equation 6, $P(CR_s)$ and $P(CR_t)$ are the distribution functions based on the probability distribution for the source and target domain CRs respectively. D^* shows the Kolmogorov-Smirnov distance between the source CR distribution and target CR distribution, i.e., it is computed as the max of distance between $P(CR_s)$ and $P(CR_t)$.

We use Two-Sample Kolmogorov-Smirnov Test (KS-Test) as a simple test for measuring the differences of the distributions of two sets, such as a sample and a reference probability distributions. Equation 6 computes the distance D^* between the medians of the Source Distribution $P(CR_s)$ and Target Distribution $P(CR_t)$. The distance D^* is the indicator that would be used to measure the CR similarity between $P(CR_s)$ and $P(CR_t)$. A larger distance D^* yields less accurate transfer learning for the target domain.

E. CR-based Inferencing

The CR-based inferencing is a mapping between the input and Class Representatives (CRs) and label it with a class. The CR-based inferencing can be done in parallel since the CRs are independent of each other.

$$\begin{aligned} \cos(CR(c), NI) &= \frac{CR(c) \cdot NI}{\|CR(c)\| \|NI\|} \\ &= \frac{\sum_{i=1}^N x_{i,c} x_{i,ni}}{\sqrt{\sum_{i=1}^N x_{i,c}^2} \sqrt{\sum_{i=1}^N x_{i,ni}^2}} \end{aligned} \quad (7)$$

Here are the steps for the CR-based inferencing. Given a new input is vectorized in the source environment to the Class Representative Feature Space (CRFS), $NI = \hat{a}(x^{(i)})$, as shown in Equation 2. The cosine similarity between the new input (NI) and Class Representatives for class c ($CR(c)$), where $c \in C$ can be computed using Equation 7. The CRL Model assigns the new input with the label associated with Class c that has the highest cosine similarity score. The higher cosine similarity score indicates the closeness between the Class Representative $CR(c)$ and the new input (NI) in the Class Representative Feature Space (CRFS).

$$\hat{c} = \operatorname{argmax}_{c \in C} \{\cos(CR(c), NI)\} \quad (8)$$

As shown in Equation 8, the label for the new input from CRL Model \hat{c} is predicted by selecting the class from all classes C that has the highest cosine similarity to the new

input. The CRL model will conduct inferencing by matching the new input against the available CRs and label it with a class having the highest cosine similarity score.

IV. IMPLEMENTATION AND EXPERIMENTAL DESIGN

The experiments on the Class Representative Learning (CRL) model have been conducted on ImageNet-1K as a source domain and CIFAR-100, CalTech-101, and CalTech-256 as a target domain. The *source* environment, i.e. the pre-trained model from the source dataset (ImageNet-1K), with three different deep learning networks, such as Inception-V3 [51], ResNet-101 [19], and VGG-19 [49].

A. Implementation

1) *System and Library Specifications*: The Feature extraction was implemented on a single GPU, which is Nvidia GeForce GTX 1080 (with 12GB GDDR5X RAM) on MATLAB 2018b version. The CR Generation and CR-based Inferencing were implemented using Spark 2.4.3 version [13]. The parallel and batch process was conducted through RDD based parallelism on a single CPU with 4GHz Intel Core i7-6700K (quad-core, 8MB cache, up to 4.2GHz with Turbo Boost) and 32GB DDR4 RAM (2,133MHz) (i.e., local parallelism of 4 cores).

2) *Models Specification*: As described in Section III-B, the *source* environment provides the feature space for the CRL model. The Inception-V3 model was predominantly used as the source environment (pre-trained with ImageNet-1K) for the CRL experiments. The Inception-V3 model was obtained from MATLAB's Pre-trained Deep Neural Networks [75]. The layer information of the Inception-V3 model is shown in Figure 6. The feature extraction has been conducted class by class as a form of parallel processing to build a CR for each class. For some experiments, ResNet-101 and VGG-19 extracted from MATLAB were also used as our source environments. The last convolution layer from the source environments was considered for Feature Extraction.

The CR Generation was implemented in parallel with Spark's Resilient Distributed Datasets (RDDs), which is a collection of features partitioned across the nodes of the cluster. The batch in this context was defined while keeping CR independence of each class for the CR Generation and CR-based Inference.

B. Datasets

We have conducted the experiments with the CRL model using four datasets according to the three transfer learning types defined in Day et al. [8], i.e., Homogeneous Transfer Learning (HOTL), Heterogeneous Transfer Learning (HETL), and Negative Transfer Learning (NTL).

- Homogeneous transfer learning happens when the source and target feature spaces have the same attributes, labels, and dimensions
- Heterogeneous transfer learning happens when the source and target domains may share no features or labels and dimensions of the feature space may differ as well

- Negative transfer learning happens when the target domain's performance negatively impacts due to knowledge transfer from the source domain. The negative transfer learning is generally found when the source domain has very little common to the target domain.

The four datasets include ImageNet-1K, CalTech-101, CalTech-256, and CIFAR-100 (as shown in Table III and Figure 4). Figure 3 shows the four datasets that were used for the CRL's transfer learning.

The source environment is built on the ImageNet-1K dataset that is the Homogeneous Transfer Learning (HOTL) type (the same label set and the same attributes). The transfer learning with CalTech-101 and CalTech-256 are the Heterogeneous Transfer Learning (HETL) type, which was projected on the semantic space of the source domain with minimal distinction classes. The transfer learning with CIFAR-100 is the Negative Transfer Learning (NTL) type since the target domain data are projected on the semantic space that is quite distinct from the source domain. Although the CIFAR-100 is semantically relevant to other datasets, the CRL space of CIFAR-100 is divergent from the source space in terms of image modality, such as image quality and image size. The size of CIFAR-100 images is [32x32] while one of the source domain ImageNet-1K [400x400]. More specifically, the dimension of the source environment of Inception-V3 is [299x299]. In the experiment section, the details on the performance of these different transfer learning types will be discussed.

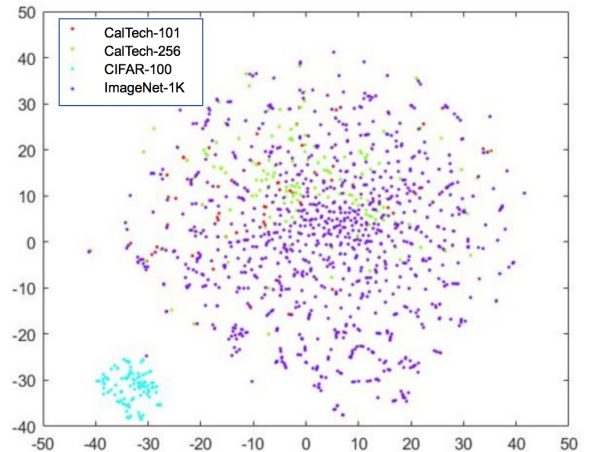


Figure 3: t-SNE Visualization of Class Representatives

Table III: Benchmark Datasets

Domain	Dataset	#Class	#Image	Image Size
Source	ImageNet-1K	1000	1,281,167	400x400
	CalTech-101	101	8,677	300x300
Target	CalTech-256	256	30,608	300x300
	CIFAR-100	100	59,917	32x32

C. Experiments for Transfer Learning Performance

Transfer Learning Performance in terms of Accuracy and Time or Space Requirements: state-of-the-art Transfer

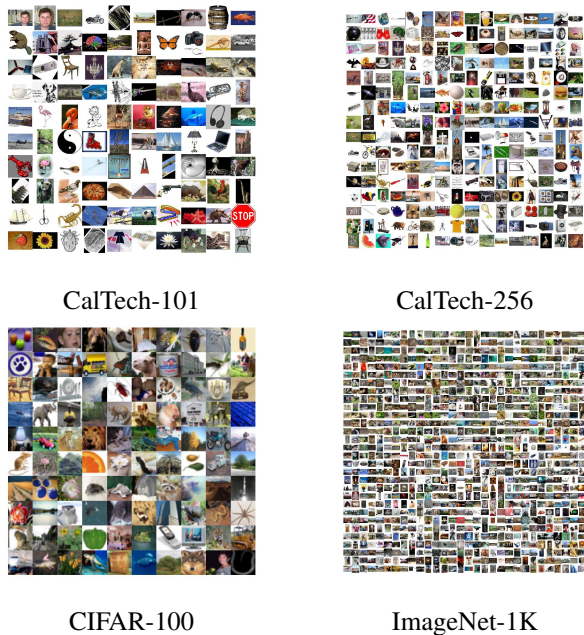


Figure 4: Benchmark Datasets: CalTech-101 & CalTech-256 & CIFAR-100 & ImageNet-1K

Learning vs. CR-based Classification with different datasets (CalTech-101, CalTech-256, ImageNet-1K, ImageNet-20K, CIFAR-100).

- Case 1: Source Domain (\mathbb{S}): ImageNet-1K, Target Domain (\mathbb{T}): CalTech-101 or CalTech-256: The distance between the medians of both domains, \mathbb{S} and \mathbb{T} , is very small (i.e., $D^* \leq 0.05$). In this case, the classification with the class representatives (CV), which are generated from the pre-trained model in \mathbb{S} with small data in \mathbb{T} , are as effective as the state-of-the-art models.
- Case 2: Source Domain (\mathbb{S}): ImageNet-1K, Target Domain (\mathbb{T}): CIFAR-100: The distance between the medians of both domains, \mathbb{S} and \mathbb{T} , is very big (i.e., $D^* \geq 0.3$) as well as the size of the data in \mathbb{T} is small.

Two-Sample Kolmogorov-Smirnov Test is used to determine whether the instances of any given class are distributed within a class. The class distribution would also be applied to determine if there are any data issues such as data labeling errors or noise data. Thus, we could estimate the class accuracy using the class distribution model even before the training. Figure 5 and Table IV shows the KS-Test results between the distribution of the source and target datasets. If the KS-Test value is high, then the source model may not be suitable for the target domain.

Figure 5 demonstrates the similarity distribution in the feature space of the source and target datasets as well as their accuracy distributions. Accuracy distribution represents the histogram of class accuracy in a given dataset while using CR based classification. Cosine similarity distribution represents the cosine similarity between a CR Pair. Higher cosine similarity means the similarity between CRs is high. The cosine similarity distribution is using to compare the *source* dataset to *target* dataset. The comparison between

CIFAR-100 and ImageNet-1K has the highest KS-Test value among the four different datasets.

The CRL model is used to understand the distribution of datasets and their performance. It also showcased the overall group cosine similarity where GCS of a class (c) is defined as the sum of cosine similarity between c and all other classes belonging to C Table V shows the CR distribution statistics for the source and target domains in terms of their accuracy and group cosine similarity (GCS). The results based on the CR-Inception-V3 as seen from Table V are consistent with Figure 3, t-SNE Visualization shows that CalTech-101 and CalTech-256 are overlapped with ImageNet-1K (source domain), while CIFAR-100 is in a long distance from the source domain. The CalTech-101 shows the best mean accuracy and low cosine similarity. However, CIFAR-100 is limited by low mean accuracy and high cosine similarity. For the CIFAR-100 dataset, the accuracy of 57.9% is the least, and the group cosine similarity of 0.74 is the highest compared to the ones for all other datasets. The salient reason for the low accuracy of the CIFAR-100 dataset is mainly due to high cosine similarity and a huge distance from the source domain. In summary, among the four datasets, CIFAR-100 performs the worst, and CalTech-101 performs the best.

D. Classification Performance with Benchmark Datasets

In this paper, the CRL model has been validated in terms of CR Feature Exaction and CR Generation as follows: i) Feature extraction in terms of CNN Network models (Inception-V3, ResNet-101) and CNN layers, ii) Feature representation and optimization such as (12K vs. 3K feature vector) and the number of training images (20, 30, 60, 100, and All). For most of the evaluation, CR-Inception-V3 version was considered.

1) *Results for Architecture Selection in Feature Extraction:* The CRs are mainly dependent on the quality of the features extracted from the pre-trained CNN model. The two popular pre-trained models such as Inception-V3 [51] and ResNet-101 [19] were used as the CR source environments and their performance was compared in Table VI. We also evaluated to select the most suitable layer in these pre-trained models. For both the pre-trained models, we compared CRL with the original accuracy, as shown in the state-of-the-art approaches ([19], [46], [51], [52], [68]).

The accuracy for the datasets reported here is for the Top-1 accuracy of the model. Comparing the CRL model to the original model, it was observed that CalTech-101 has an increase of 1.56% in both the models. There was a significant decrease in the accuracy of The CIFAR-100 for both the models. This is likely due to the greater distance in a semantic space between the source domain (ImageNet-1K) and the target domain (CIFAR-100), as discussed in Section IV-B. In the end, for the overall comparison of the models, the accuracies of the Homogeneous Transfer Learning (HTL) in Inception-V3 are better than the ones in ResNet-101. This comparison leads to the use of Inception-V3 as the source environment of the CRL model.

2) *Results for Layer Selection in Feature Extraction:* From Inception-V3, the most suitable layer for the Feature

Table IV: Source Domain and Target Domain: Cosine Similarity Median, Accuracy, Kolmogorov-Smirnov Test Scores
 *CS: Cosine Similarity. A high CS Distance ($S_m - T_m$) and high KS Test Score indicate Negative Transfer Learning.
 State-of-the-Accuracy is from Inception-V3 Model (Refer Table VI)

Source Domain			Target Domain				Source & Target Comparison		
Dataset	CS Median (S_m)	Accuracy (S_a)	Dataset	CS Median (T_m)	Accuracy (T_a)	State-of-the-art Accuracy (SA_a)	CS Distance ($S_m - T_m$)	KS Test Score	Accuracy Change ($SA_a - T_a$)
ImageNet-1K	0.434	73.9%	CalTech-101	0.398	93.9%	92.98%	0.036	0.1570	+1%
ImageNet-1K	0.434	73.9%	CalTech-256	0.454	77.9%	77.6%	0.02	0.0921	+0.3%
ImageNet-1K	0.434	73.9%	CIFAR-100	0.734	57.9%	76.2%	0.3	0.9125	-18.3%
ImageNet-1K	0.434	73.9%	ImageNet-1K	0.434	73.9%	78.8%	0	0	-4.9%

Table V: Class Representative Distribution Statistics

	CIFAR-100		CalTech-101		CalTech-256		ImageNet-1K	
	Accuracy	GCS	Accuracy	GCS	Accuracy	GCS	Accuracy	GCS
Mean Accuracy	57.9%	0.74	88.8%	0.41	76.0%	0.46	73.8%	0.43
Std dev	15.2%	0.09	9.7%	0.13	15.6%	0.11	12.9%	0.10
Range	[17.7%, 86.4%]	[0.44, 0.98]	[55.6%, 100%]	[0.03, 0.92]	[29.1%, 100%]	[0.08, 0.96]	[28.6%, 96.5%]	[0, 0.99]

GCS: Group Cosine Similarity

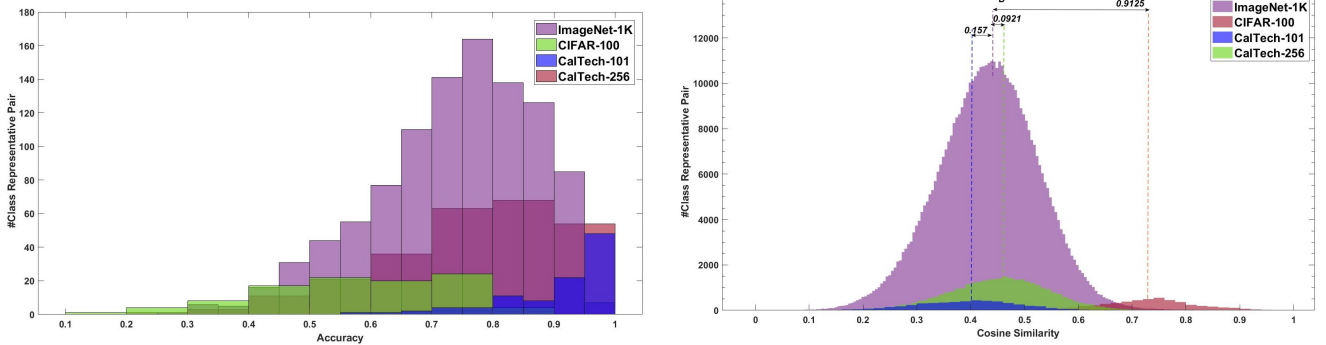


Figure 5: Accuracy Distribution and Cosine Similarity Distribution

Table VI: CRL Models based on Deep Learning Networks (Inception-V3 vs. ResNet-101)

Base Model	Inception-V3		ResNet-101	
	CRL Model	State-of-the-Art Model [51]	CRL Model	State-of-the-Art Model [19]
Parameter	0	21.8M	0	22.44M [68]
Feature	3072	2048	100352	2048
Shape	AvgPool([8x8x192])	linear [1x1x2048]	[7x7x2048]	linear [1x1x2048]
Layer	conv2d_94	48 layers deep (347 layers)	res5c_branch2c	101 layers deep (316 layers)
ImageNet-1K	74.07%	78.8%	68.4%	77.56% [68]
CalTech-101	93.69%	92.88%	93.46%	91.4% [52]
CalTech-256	77.78%	77.6%	76.76%	80.1% [52]
CIFAR-100	57.63%	76.2%	63.02%	72.77% [46]

Extraction was identified by the layer-wise experiment. As shown in Table VII, the accuracy evaluation was conducted with the models built using the features from the selected layer. For this comparison, the twelve layers (including ten different convolution layers, final concatenated convolution layer, and final average pooling layer) were considered. These layers are indexed, as shown in Figure 6.

The best layer was determined in terms of the feature size and the accuracy of the model. Table VII shows the feature size, flatten feature size, and accuracy. For this evaluation, comparable datasets are considered to evaluate the effectiveness of the CR-based classification. The Homogeneous

Transfer Learning (HTL) was used to conduct non-biased feature analysis and layer selection. Layer 10 (conv2d-94) shows the best accuracy in CalTech-101, while Layer 12 (AvgPool) shows the best accuracy in CalTech-256. For the flatten feature size, the feature set of Layer 10 shows the highest accuracy compare to other layers.

3) *Results from Feature Reduction*: Once the CR feature map is generated, the CRL model might be required to compress it for mobile deployment. In this paper, we have applied three different sampling techniques for the model compression: (1) Max Pooling, (2) Average Pooling, and (3) Min Pooling. The Max Pooling is a sample-based discretization technique

that is widely used in Deep Learning. The objective of the Max Pooling is to reduce the feature map’s dimensionality by applying the max operation to features contained in the sub-regions of the feature map. The initial input of the CR feature map, such as $X * X$ matrix (e.g., $8*8$), will produce to $Y * Y$ matrix (e.g., $4*4$) using a $Z*Z$ filter (e.g., $2*2$). A stride of S (e.g., 2) controls how the filter operates around the input matrix by shifting S units at a time without any overlap regions.

For each of the regions represented by the filter, the max of that region is computed to create the output feature map, in which each element is the max of a region in the original input. The Average Pooling and Min Pooling are very similar to the Max Pooling; the only difference is to utilize a different operation such as average and min operations for the feature map reduction.

Considering the feature size of the Layer 10 in Inception-V3, we evaluate by reducing the dimensions using standard reduction techniques, namely minimum pooling (MinPool), maximum pooling (MaxPool), and average pooling (AvgPool). The pooling in CBL was implemented on the $[8x8,192]$ feature vector (Layer 10) with the filter size of $2x2$ transforming into $[4x4,192]$. In CR-Inception-V3C, we applied AvgPool with a filter size $[2x2]$ to the feature map of $[8x8x192]$ extracted from Layer 10 and obtained the reduced feature map of $[4x4x192]$. As shown in Figure 7, the average pooling layer reduction is applied to the post-processing of CR-Generation. The same filter size was used for MaxPool and MinPool.

Table VIII shows the accuracy for CR-Inception-V3C by using the filter size based on the three pooling techniques. Based on the analysis with all of the datasets, CR-Inception-AvgPool showed the accuracy drop with an average of 1% in Top-1 accuracy when comparing with 12K or the original Layer 10 Accuracy. The interesting observation through this evaluation was the 12K CRL model’s Top-5 Accuracy outperformed on all datasets compared with other available models.

4) *Results from Data Imbalance Experiments:* Most of the deep learning suffered from the data imbalance problem. Our experiments show that CRL is not sensitive to the data imbalance issue. Since CalTech-101 and CalTech-256 are imbalanced datasets, we have conducted experiments to show their classification performance is independent of the number of input.

In order to analyze the imbalanced data issue in the CRL model, we have evaluated the CR Generation with a varying number of images and accuracy. As Table IX shows the CR Generation accuracy for the image sets of 20, 30, 60, 100 and all. All represented in the training dataset (i.e., 70%) for any given class. The results show that the accuracy of CR-based classification does not vary significantly for a varying number of images. This effect is clearly shown with the imbalanced datasets such as CalTech-101 and CalTech-256. For example, CalTech-101, Class *airplanes* have 560 images with the class accuracy of 97.9% while *camera* has 35 images with the class accuracy of 96.8%. This indicates that the image imbalance problem does not affect the classification accuracy in the CRL model.

E. Model Performance Comparison

The CRL model’s performance is evaluated by comparing with Inception-V3 pre-trained model retrained with the target domain. The CRL model’s performance is calculated based on AFM Generation Time (refer to Section III-B), CR-based Inference Time (refer to Section III-E) and CR Model Generation Time (refer to Section III-C).

Table X shows the comparison of the CRL model’s overall time vs. the time taken for retraining the dataset using the Inception-V3 pre-trained model. The pre-trained model was run on the same system specification as the CRL model. Pre-training of the Inception-V3 Model was stopped at a reported number of epochs as the time taken was significantly higher than that of the CRL model. The CRL model with three datasets, (CalTech-101, CalTech-256, and CIFAR-100) have an average of 99% time reduction that is a significantly reduced time compared with that for the original Inception-V3 model. Within the same time window and based on the same pre-trained model, the Inception-V3 model performance has not reached the accuracy published in [26]. The CRL model’s overall time shows genuinely outstanding performances in the target domains, even if the models never learned from the target domain.

F. Comparison with Lightweight Classification Models

The two CRL models, namely CR-Inception-V3 [based on 12K Layer 10] (refer to Figure 6) and CR-Inception-V3C [based on AvgPool] (refer to Figure 7) were considered for evaluation. The CRL models are compared with the state-of-the-art mobile Deep Learning models such as Mobile-Net-v1 [20], Mobile-Net-v2 [45] and NasNet-Mobile [73]. The Inception-V3 Model accuracy is also compared as the CRL model is based on Inception-V3 (refer to Section IV-D). The state-of-the-art accuracies shown in XI were based on the work by Kornblith et al. [26]. The another work by Kornblith et al. [48] was based on the performance of checkpoints from TensorFlow-Slim repository.

The following a brief review of Light-Weight Classification models that are compared with CRL.

- **MobileNet-v1** MobileNet-v1 is one of pioneer work in light-weight convolution neural network. A efficient low latency model is achieved using Depthwise Convolution Filters [20]
- **MobileNet-v2** MobileNet-v2 is extension of MobileNet-v1, they improve light-weight model using inverted residual module with linear bottleneck. MobileNet-v2 1.4 is a version with neural network image input size of $224x224$ and multipliers set to 1.4 [45].
- **NASNet-A-Mobile** NASNet is Convolution Neural Network where the Semantic Space is transferred from smaller dataset to bigger dataset using a Reinforcement Learning Search Method called Neural Architecture Search (NAS) [73].

The comparison between the mobile models and CRL is conducted in terms of the computational cost, model size, and accuracy. The computation cost is usually defined based on floating-point operations (FLOPs) and parameters. The FLOPs

Table VII: Inception-V3 Layerwise Accuracy on Similar Domain Datasets (SID)

Num	Layer	Filter Size	Activation Shape	Activation Size	CalTech-101	CalTech-256
1	conv2d_10	3x3x64	35x35x96	117601	59.9%	24.0%
2	conv2d_20	1x1x288	35x35x64	78401	52.7%	23.7%
3	conv2d_30	3x3x96	17x17x96	27745	71.3%	32.0%
4	conv2d_40	1x1x768	17x17x192	55489	79.0%	44.1%
5	conv2d_50	1x1x768	17x17x192	55489	79.7%	47.1%
6	conv2d_60	1x1x768	17x17x192	55489	83.8%	52.2%
7	conv2d_70	1x1x768	17x17x192	55489	81.1%	49.5%
8	conv2d_80	3x1x384	8x8x384	24577	93.3%	74.2%
9	conv2d_90	1x1x2048	8x8x448	28673	85.3%	62.1%
10	conv2d_94	1x1x2048	8x8x192	12289	94.4%	78.2%
11	mixed10	-	8x8x2048	131073	91.9%	77.9%
12	avg-pool	8x8 [pooling]	1x1x2048	2049	90.0%	79.1%

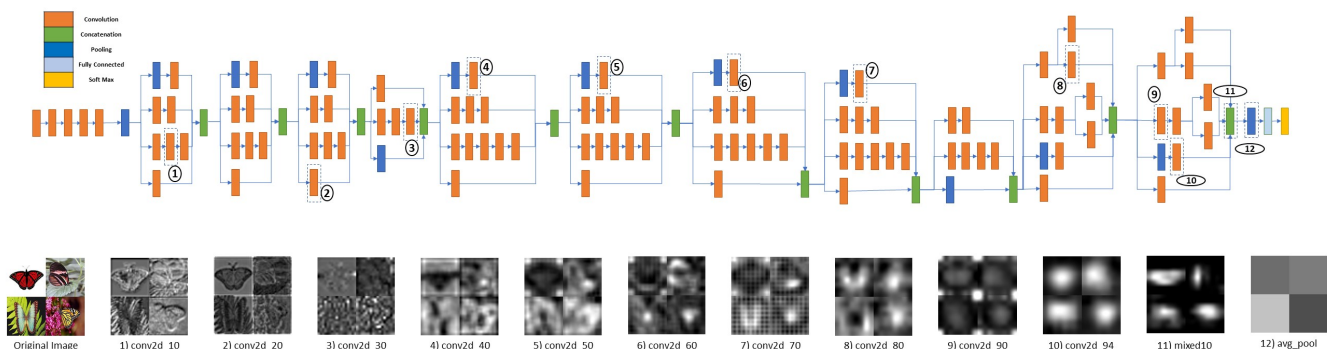


Figure 6: Inception-V3 Activation Visualization Layerwise

Table VIII: Feature Pooling and Top Accuracy
12K: Original; AVP: Average Pooling; MIP: Min Pooling; MAP: Max Pooling

	ImageNet-1K				CalTech-101				CalTech-256				CIFAR-100			
	12K	AVP	MIP	MAP	12K	AVP	MIP	MAP	12K	AVP	MIP	MAP	12K	AVP	MIP	MAP
Feature#	12288	3072	3072	3072	12288	3072	3072	3072	12288	3072	3072	3072	12288	3072	3072	3072
Top 1	73.93	74.07	72.47	70.12	93.96	93.69	93.46	91.89	77.87	77.78	74.83	71.14	57.96	57.63	55.76	55.25
Top 2	83.7	83.89	81.92	79.73	97.23	97.23	97.08	96.04	84.59	84.6	81.75	78.31	70.61	70.38	68.73	67.95
Top 5	93.31	90.56	88.41	86.59	99.15	98.73	98.42	97.89	92.43	89.83	86.99	84.37	90.5	83.42	81.89	81.48

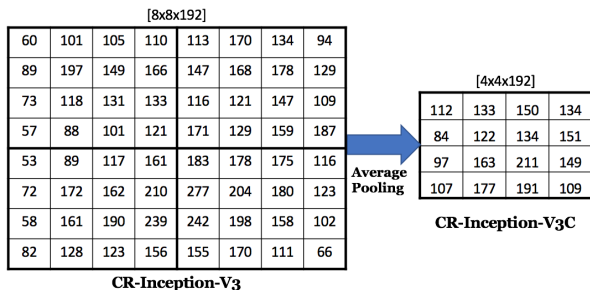


Figure 7: Average Pooling is applied; 8x8 sized 192 channels [8x8x192] are reduced to 4x4 sized 192 channels [4x4x192]

of the CRL model are less than the one for prediction with the base model, i.e., Inception-V3. As shown in Table XI, the number of parameters for the CRL model is Nil as there is no

Table IX: Image Classification Accuracy for an Increasing Image#

Dataset	Image Count & Accuracy				
	20	30	60	100	All
ImageNet-1K	69.5%	70.9%	72.5%	73.0%	73.9%
CalTech-101	91.9%	93.5%	93.6%	93.8%	93.9%
CalTech-256	74.4%	75.8%	77.3%	77.8%	77.9%
CIFAR-100	50.9%	53.4%	55.9%	56.8%	57.9%

traditional learning component in the CRL model. The CRL model's computational cost outperforms all the other models.

The CRL model's size is given based on the size of each CRL of class. The significant difference between the traditional deep learning model and the CRL model is that the model size is dependent on the number of classes rather than the number of layers or size of the layer. The size as listed in Table XI, includes two parts the size of the pre-trained model

Table X: Transfer Learning Performance Analysis: CRL vs. Inception-V3 [75]
Pretrained Model: Inception-V3 with ImageNet-1K

Domain		CRL				Inception-V3 [75]		
Source	Target	Step	Time	Overall Time	Accuracy	Time	Epoch	Accuracy
ImageNet-1K	CalTech-101	AFM Generation	5m 21s	7m 12s	94.40%	4257m 55s	40 Epochs	88.73%
		CR Model Generation	1m 31s					
		CR Inferencing	20s					
	CalTech-256	AFM Generation	10m 14s	13m 53s	78.20%	14193m 58s	14 Epochs	59.26%
		CR Model Generation	1m 54s					
		CR Inferencing	1m 45s					
	CIFAR-100	AFM Generation	13m 12s	15m 44s	57.96%	26941m 51s	10 Epochs	50.30%
		CR Model Generation	56s					
		CR Inferencing	1m 36s					

plus the per CR per class size, i.e., 0.15MB for CR-Inception-V3 and 0.06MB for CR-Inception-V3C.

In Table XI, the two CRL models were compared with other mobile models. These models outperform the existing mobile models. Also, these models perform better than the original Inception model with CalTech-101 and CalTech-256 datasets. Their performances are reasonably comparable to the original ones with ImageNet-1K Dataset. However, the CRL models do not perform well on the CIFAR-100 Dataset. Overall, the CRL models are better than state-of-the-art mobile models if the target domains are similar to the source models. Otherwise, as seen from the CIFAR-100 model, the performance did not meet expectations. It is because there is a considerable gap between the source and target domains, and this gap may result from the lack of learning in the target domain.

This result confirms that the CRL model can be used to validate the distribution of data in terms of dissimilarities and similarities of CRs. The classification accuracy can be estimated based on the CR distribution model. Furthermore, outliers of data can be normalized, or mislabeled images can be detected with a CR.

G. Comparison with Zero-Shot Learning Algorithms

In this section, we evaluate the CRL model using three different evaluations; Recognition Task-based Accuracy, Accuracy with an increasing number of instances of the unseen dataset, and comparison with state-of-the-art Zero-Shot Learning (ZSL) approach. For this section, we consider two versions of the CRL model; (i) Inception-V3 based and (ii) VGG-19 based model. In Tables XII and XIII, the performance of Inception-V3 model-based CRL (CR-Inception-V3) in the ZSL perspectives was presented.

The CRL model is capable of recognizing the target labels (unseen data) without having the source labels (seen data) as an option. This shows the advantage and ability as a classification model (see Section IV-F). Table XII shows two versions of the recognition tasks with testing data from target set (\mathbb{T}); $\mathbb{T} \Rightarrow \mathbb{T}$ when the testing label could be only from the target set $y^* \in \mathbb{T}$ and $\mathbb{T} \Rightarrow \mathbb{S} \cup \mathbb{T}$ when the testing label could be from both the source set and target set $y^* \in \mathbb{S} \cup \mathbb{T}$. For this experiment, we consider all instances (70% of the dataset) from the dataset to generate CRs. The increase in the number of labels in the dataset was compared with the

accuracy. There were significant drops when the source set was also considered. The interesting observation is that the Heterogeneous Domain (HD) such as CIFAR-100 does not have a significant drop in accuracy, which makes sense, as CIFAR-100's CR space does not overlap with ImageNet-1K's CR space (see Figure 3).

Table XIII shows the performance of CR-Inception-V3 with one image from each class to ten images from each class. For this experiment, we considered only ($\mathbb{T} \Rightarrow \mathbb{T}$) setting. The interesting to see that the CRL model with just ten images from each class all the dataset Top-1 accuracy reach more than 75% of accuracy achieved when all instances are used.

Table XIV shows the comparison of state-of-the-art Zero-Shot Learning methods briefly introduced in Table I. The following is a brief review of the ZSL models, which are compared with CRL.

- **Deep WMM-Voc:** Deep Weight Maximum Margin Vocabulary (Deep WMM-Voc) is Classifier-based ZSL, which uses a joint embedding for visual features and semantic words. The results generated for this comparison done based on the same settings proposed in this work [15], [16].
- **SAE:** Semantic Auto-Encoder (SAE) is an encoder-decoder paradigm that projects visual features into semantic representation spaces such as Attribute Space and use the decoder to reconstruct the original visual features [24].
- **ESZSL & Deep-SVR:** ESZSL and Deep-SVR are an Attribute Space-based ZSL model. ESZSL implements a linear model together with regularizers for attribute learning, whereas Deep-SVR uses a probabilistic attribute classifier [29], [43].
- **Embed:** Embed is Instance-Based ZSL using Label Embedding Space. Embed uses Multi-modal fusion semantic representation with RNN [69].
- **DeViSE & ConSE:** DeVISE and ConSE are Label Embedding Space-based ZSL Models. Both benefit from Convolution Neural Networks, where DeVISE uses Soft-Max Classifier, and ConSE uses a ranking algorithm for prediction [14], [33].
- **AMP:** AMP is a Label Embedding Space-based ZSL model. Absorbing Markov Chain Process is formulated on a semantic graph that provides processing efficiency in ZSL [17].

Table XI: Comparison of Class Representative with Pre-trained Models([26], [74])

Model	Parameters ^a	Feature Size	Image Size	Model Size	Accuracy			
					ImageNet-1K	CalTech256	CalTech101	CIFAR100
MobileNet-V1 [20]	3.2M	1024	224	16MB	70.6%	N/A	90.7%	70.9%
MobileNet-V2 [45]	2.2M	1280	224	13MB	72%	N/A	91.26%	70.6%
MobileNet-V2 (1.4) [45]	4.3M	1792	224	24MB	74.7%	N/A	91.83%	73.4%
NASNet-A Mobile [73]	4.2M	1056	224	20MB	74%	N/A	91.52%	73.6%
Inception-V3 [51]	21.8M	2048	299	89MB	78.8%	N/A	92.98%	76.2%
CR-Inception-V3 (ours)	N/A	12288	299	0.15MB/CR*	73.93%	77.87%	93.96%	57.96%
CR-Inception-V3C (ours)	N/A	3072	299	0.06MB/CR*	74.07%	77.78%	93.69%	57.63%

* CR-Inception-V3 uses Inception-V3 as its pre-trained model, which is 89MB.

Table XII: Accuracy for CR-Inception-V3 Zero-Shot Learning Tasks

Dataset	Recognition Task Accuracy		
	Accuracy	T \Rightarrow T	T \Rightarrow S \cup T
CalTech-101	Top 1	93.9%	87.4%
	Top 5	99.1%	97.5%
CalTech-256	Top 1	77.8%	40.9%
	Top 5	92.4%	54.9%
CIFAR-100	Top 1	57.9%	57.4%
	Top 5	90.5%	83.4%

Table XIII: CR-Inception-V3 Accuracy with Increasing Target Instances (#Ins.)

#Ins.	CalTech-101		CalTech-256		CIFAR-100		ImageNet-1K	
	T-1	T-5	T-1	T-5	T-1	T-5	T-1	T-5
1	70.2	83.4	41.4	54.8	20	38	32.5	50.1
2	79.2	92.3	51.7	66.7	25.5	52.2	44	64.9
3	85.3	95.2	56.5	72.1	30.3	56.9	50.9	72.3
4	85.6	96.7	61.5	77.1	36	62.9	54.9	76.2
5	86.8	97	63.6	78	38	66.7	58.1	79
6	87	97.6	65.1	79.4	40.9	69.5	60.3	81.2
7	89.4	97.7	67.2	82.2	42.4	70.8	61.3	82.2
8	90.7	98	68.2	82.4	44.6	73.6	63.4	83.6
9	90.8	97.9	69.8	83.8	44.8	74.1	64.6	84.6
10	91.2	98.2	70	84.4	45.8	75.4	65.4	85.2
all	93.9	99.1	77.8	92.4	57.9	90.5	73.9	93.3

Table XIV shows that the performance of the CRL model is superior in both cases, with 3000 instances and all instances. In the case of the 3000 instances, the CRL model’s Top-1 has a 27% increase from the top performer, Deep WMM-Voc. In the case of all instances, the CRL model’s Top-1 is significantly higher than others; on average, the CRL model’s Top-1 accuracy is 3 times higher than Deep WMM-Voc’s.

V. DISCUSSION

The limitations of the CRL model are that a source environment (except the fully connected layers) is still required for generating a feature map for any input in the testing. The size of the source environment may be too big to fit in low-end devices like mobile devices. In our research, we can provide a cloud service for the feature map generation as a basic interface, such as Application Programming Interfaces (APIs) for lightweight mobile applications.

The Class Representative (CR) generation was obtained by extracting the abstraction of the distribution of each feature in

Table XIV: Comparison between the CRL model with VGG-19/ImageNet-1K and State-of-the-art ZSL Models

Methods	3000 Instances		All Instances	
	Top-1	Top-5	Top-1	Top-5
CRL with VGG-19 (ours)	11.78	25.52	31.6	55.1
Deep WMM-Voc [15], [16]	9.26	21.99	10.29	23.12
SAE [24]	5.11	12.26	9.32	21.04
ESZSL [43]	5.86	13.71	8.3	18.2
Deep-SVR [29]	5.29	13.32	5.7	14.12
Embed [69]	-	-	11.00	25.7
ConSE [33]	5.5	13.1	7.8	15.5
DeViSE [14]	3.7	11.8	5.2	12.8
AMP [17]	3.5	10.5	6.1	13.1

*Results reported for SOTA Models are from Fu et al. [16]. The CRL model is configured with the same settings such as VGG-19 with 3000 instances i.e., 3 images per class and all 50000 instances i.e., 50 images per class

the Class Representative Feature Space (CRFS) of an input image. For the purpose, we used a simple average mean approach. Thus, a CR can be sensitive to outliers and sample size bias of the CRFS. The CRL model was extremely strong at the Top-5 inferencing compared to Top-1 inferencing (see Table VIII). The CR computation might not be accurate due to bias or unexpected outliers. This indicates that the high similarity between some CRs can lead to misclassification. To overcome the limitation of the CR Generation, We will explore an advanced optical model such as the Fisher Vector and Gaussian-Mixture-Model. We also can use unsupervised deep learning techniques such as the autoencoder in learning efficient data codings to reduce the CR’s Feature Space to a more optimal representation. We can further extend it to determine the common and unique features of the CR vectors and find the weights that maximize the uniqueness between CRs.

VI. CONCLUSION

We presented the Class Representative Learning (CRL) model that is based on class-level classifiers, built class-by-class, that would be a representative of instances of a specific class by utilizing activation features of Convolutional Neural Networks responding to the new cases. The characteristics of the CRL are high efficiency, being compact and lightweight. It was possible because the CRs can be generated in a parallel and distributed manner, and the inferencing can be conducted through matching new inputs with CRs. Comprehensive evaluations have been conducted with the CRL model, compared

to the state-of-the-art approaches both in classification and zero-shot learning using the four benchmark datasets. The CRL model was shown to increase accuracy and reduce considerable times in building CNN based classifiers.

VII. ACKNOWLEDGMENT

This work was partially supported by NSF CNS #1747751 and CNS #1650549.

REFERENCES

- [1] Zeynep Akata, Mateusz Malinowski, Mario Fritz, and Bernt Schiele. Multi-cue zero-shot learning with strong supervision. In *Proceedings of the IEEE Conference on Computer Vision and Pattern Recognition*, pages 59–68, 2016.
- [2] Zeynep Akata, Florent Perronnin, Zaid Harchaoui, and Cordelia Schmid. Label-embedding for image classification. *IEEE transactions on pattern analysis and machine intelligence*, 38(7):1425–1438, 2015.
- [3] Yonatan Amit, Michael Fink, Nathan Srebro, and Shimon Ullman. Uncovering shared structures in multiclass classification. In *Proceedings of the 24th international conference on Machine learning*, pages 17–24. ACM, 2007.
- [4] Evgeniy Bart and Shimon Ullman. Cross-generalization: Learning novel classes from a single example by feature replacement. In *2005 IEEE Computer Society Conference on Computer Vision and Pattern Recognition (CVPR'05)*, volume 1, pages 672–679. IEEE, 2005.
- [5] Abhijit Bendale and Terrance Boulton. Towards open world recognition. In *Proceedings of the IEEE Conference on Computer Vision and Pattern Recognition*, pages 1893–1902, 2015.
- [6] Hakan Bilen and Andrea Vedaldi. Universal representations: The missing link between faces, text, planktons, and cat breeds. *arXiv preprint arXiv:1701.07275*, 2017.
- [7] Alfredo Canziani, Adam Paszke, and Eugenio Culurciello. An analysis of deep neural network models for practical applications. *arXiv preprint arXiv:1605.07678*, 2016.
- [8] Oscar Day and Taghi M Khoshgoftaar. A survey on heterogeneous transfer learning. *Journal of Big Data*, 4(1):29, 2017.
- [9] P Kingma Diederik, Max Welling, et al. Auto-encoding variational bayes. In *Proceedings of the International Conference on Learning Representations (ICLR)*, 2014.
- [10] Jeff Donahue, Yangqing Jia, Oriol Vinyals, Judy Hoffman, Ning Zhang, Eric Tzeng, and Trevor Darrell. Decaf: A deep convolutional activation feature for generic visual recognition. In *International conference on machine learning*, pages 647–655, 2014.
- [11] Ali Farhadi, Ian Endres, Derek Hoiem, and David Forsyth. Describing objects by their attributes. In *2009 IEEE Conference on Computer Vision and Pattern Recognition*, pages 1778–1785. IEEE, 2009.
- [12] Francois Fleuret and Gilles Blanchard. Pattern recognition from one example by chopping. In *Advances in Neural Information Processing Systems*, pages 371–378, 2006.
- [13] Apache Software Foundation. Apache spark. (Accessed on 05/26/2019).
- [14] Andrea Frome, Greg S Corrado, Jon Shlens, Samy Bengio, Jeff Dean, Marc’Aurelio Ranzato, and Tomas Mikolov. Devise: A deep visual-semantic embedding model. In *Advances in neural information processing systems*, pages 2121–2129, 2013.
- [15] Yanwei Fu and Leonid Sigal. Semi-supervised vocabulary-informed learning. In *Proceedings of the IEEE Conference on Computer Vision and Pattern Recognition*, pages 5337–5346, 2016.
- [16] Yanwei Fu, Xiaomei Wang, Hanze Dong, Yu-Gang Jiang, Meng Wang, Xiangyang Xue, and Leonid Sigal. Vocabulary-informed zero-shot and open-set learning. *IEEE transactions on pattern analysis and machine intelligence*, 2019.
- [17] Zhenyong Fu, Tao Xiang, Elyor Kodirov, and Shaogang Gong. Zero-shot object recognition by semantic manifold distance. In *The IEEE Conference on Computer Vision and Pattern Recognition (CVPR)*, June 2015.
- [18] Kaiming He, Ross Girshick, and Piotr Dollár. Rethinking imagenet pre-training. *arXiv preprint arXiv:1811.08883*, 2018.
- [19] Kaiming He, Xiangyu Zhang, Shaoqing Ren, and Jian Sun. Deep residual learning for image recognition. In *Proceedings of the IEEE conference on computer vision and pattern recognition*, pages 770–778, 2016.
- [20] Andrew G Howard, Menglong Zhu, Bo Chen, Dmitry Kalenichenko, Weijun Wang, Tobias Weyand, Marco Andreetto, and Hartwig Adam. Mobilenets: Efficient convolutional neural networks for mobile vision applications. *arXiv preprint arXiv:1704.04861*, 2017.
- [21] Gao Huang, Zhuang Liu, Laurens Van Der Maaten, and Kilian Q Weinberger. Densely connected convolutional networks. In *Proceedings of the IEEE conference on computer vision and pattern recognition*, pages 4700–4708, 2017.
- [22] Ashish Kapoor, Bongshin Lee, Desney Tan, and Eric Horvitz. Learning to learn: Algorithmic inspirations from human problem solving. In *Twenty-Sixth AAAI Conference on Artificial Intelligence*, 2012.
- [23] Durk P Kingma, Shakir Mohamed, Danilo Jimenez Rezende, and Max Welling. Semi-supervised learning with deep generative models. In *Advances in neural information processing systems*, pages 3581–3589, 2014.
- [24] Elyor Kodirov, Tao Xiang, and Shaogang Gong. Semantic autoencoder for zero-shot learning. In *Proceedings of the IEEE Conference on Computer Vision and Pattern Recognition*, pages 3174–3183, 2017.
- [25] Iasonas Kokkinos. Ubernet: Training a universal convolutional neural network for low-, mid-, and high-level vision using diverse datasets and limited memory. In *Proceedings of the IEEE Conference on Computer Vision and Pattern Recognition*, pages 6129–6138, 2017.
- [26] Simon Kornblith, Jonathon Shlens, and Quoc V Le. Do better imagenet models transfer better? *arXiv preprint arXiv:1805.08974*, 2018.
- [27] Brenden Lake, Ruslan Salakhutdinov, Jason Gross, and Joshua Tenenbaum. One shot learning of simple visual concepts. In *Proceedings of the Annual Meeting of the Cognitive Science Society*, volume 33, 2011.
- [28] Christoph H Lampert, Hannes Nickisch, and Stefan Harmeling. Learning to detect unseen object classes by between-class attribute transfer. In *2009 IEEE Conference on Computer Vision and Pattern Recognition*, pages 951–958. IEEE, 2009.
- [29] Christoph H Lampert, Hannes Nickisch, and Stefan Harmeling. Attribute-based classification for zero-shot visual object categorization. *IEEE Transactions on Pattern Analysis and Machine Intelligence*, 36(3):453–465, 2013.
- [30] Aravindh Mahendran and Andrea Vedaldi. Understanding deep image representations by inverting them. In *Proceedings of the IEEE conference on computer vision and pattern recognition*, pages 5188–5196, 2015.
- [31] Tomas Mikolov, Ilya Sutskever, Kai Chen, Greg S Corrado, and Jeff Dean. Distributed representations of words and phrases and their compositionality. In *Advances in neural information processing systems*, pages 3111–3119, 2013.
- [32] Kaiming Nan, Sicong Liu, Junzhao Du, and Hui Liu. Deep model compression for mobile platforms: A survey. *Tsinghua Science and Technology*, 24(6):677–693, 2019.
- [33] Mohammad Norouzi, Tomas Mikolov, Samy Bengio, Yoram Singer, Jonathon Shlens, Andrea Frome, Greg S Corrado, and Jeffrey Dean. Zero-shot learning by convex combination of semantic embeddings. *arXiv preprint arXiv:1312.5650*, 2013.
- [34] Mark Palatucci, Dean Pomerleau, Geoffrey E Hinton, and Tom M Mitchell. Zero-shot learning with semantic output codes. In *Advances in neural information processing systems*, pages 1410–1418, 2009.
- [35] Sinno Jialin Pan, Qiang Yang, et al. A survey on transfer learning. *IEEE Transactions on knowledge and data engineering*, 22(10):1345–1359, 2010.
- [36] Deepak Pathak, Ross Girshick, Piotr Dollár, Trevor Darrell, and Bharath Hariharan. Learning features by watching objects move. In *Proceedings of the IEEE Conference on Computer Vision and Pattern Recognition*, pages 2701–2710, 2017.
- [37] Jeffrey Pennington, Richard Socher, and Christopher Manning. Glove: Global vectors for word representation. In *Proceedings of the 2014 conference on empirical methods in natural language processing (EMNLP)*, pages 1532–1543, 2014.
- [38] Rajat Raina, Alexis Battle, Honglak Lee, Benjamin Packer, and Andrew Y Ng. Self-taught learning: transfer learning from unlabeled data. In *Proceedings of the 24th international conference on Machine learning*, pages 759–766. ACM, 2007.
- [39] Sachin Ravi and Hugo Larochelle. Optimization as a model for few-shot learning. In *International Conference on Learning Representations*, 2016.
- [40] Sylvestre-Alvise Rebuffi, Hakan Bilen, and Andrea Vedaldi. Learning multiple visual domains with residual adapters. In *Advances in Neural Information Processing Systems*, pages 506–516, 2017.
- [41] Sylvestre-Alvise Rebuffi, Hakan Bilen, and Andrea Vedaldi. Efficient parametrization of multi-domain deep neural networks. In *Proceedings of the IEEE Conference on Computer Vision and Pattern Recognition*, pages 8119–8127, 2018.

- [42] Danilo Jimenez Rezende, Shakir Mohamed, Ivo Danihelka, Karol Gregor, and Daan Wierstra. One-shot generalization in deep generative models. *arXiv preprint arXiv:1603.05106*, 2016.
- [43] Bernardino Romera-Paredes and Philip Torr. An embarrassingly simple approach to zero-shot learning. In *International Conference on Machine Learning*, pages 2152–2161, 2015.
- [44] Olga Russakovsky, Jia Deng, Hao Su, Jonathan Krause, Sanjeev Satheesh, Sean Ma, Zhiheng Huang, Andrej Karpathy, Aditya Khosla, Michael Bernstein, Alexander C. Berg, and Li Fei-Fei. ImageNet Large Scale Visual Recognition Challenge. *International Journal of Computer Vision (IJCV)*, 115(3):211–252, 2015.
- [45] Mark Sandler, Andrew Howard, Menglong Zhu, Andrey Zhmoginov, and Liang-Chieh Chen. Mobilenetv2: Inverted residuals and linear bottlenecks. In *Proceedings of the IEEE Conference on Computer Vision and Pattern Recognition*, pages 4510–4520, 2018.
- [46] Anish Shah, Eashan Kadam, Hena Shah, Sameer Shinde, and Sandip Shingade. Deep residual networks with exponential linear unit. *arXiv preprint arXiv:1604.04112*, 2016.
- [47] Li Shen, Gang Sun, Qingming Huang, Shuhui Wang, Zhouchen Lin, and Enhua Wu. Multi-level discriminative dictionary learning with application to large scale image classification. *IEEE Transactions on Image Processing*, 24(10):3109–3123, 2015.
- [48] N. Silberman and S. Guadarrama. Tensorflow-slim image classification model library. <https://github.com/tensorflow/models/tree/master/research/slim>, 2016. (Accessed on 08/19/2019).
- [49] Karen Simonyan and Andrew Zisserman. Very deep convolutional networks for large-scale image recognition. *arXiv preprint arXiv:1409.1556*, 2014.
- [50] Jake Snell, Kevin Swersky, and Richard Zemel. Prototypical networks for few-shot learning. In *Advances in Neural Information Processing Systems*, pages 4077–4087, 2017.
- [51] Christian Szegedy, Vincent Vanhoucke, Sergey Ioffe, Jon Shlens, and Zbigniew Wojna. Rethinking the inception architecture for computer vision. In *Proceedings of the IEEE conference on computer vision and pattern recognition*, pages 2818–2826, 2016.
- [52] Youssef Tamaazousti, Hervé Le Borgne, and Céline Hudelot. Mucanet: Multi categorical-level networks to generate more discriminating features. In *Proceedings of the IEEE Conference on Computer Vision and Pattern Recognition*, pages 6711–6720, 2017.
- [53] Youssef Tamaazousti, Hervé Le Borgne, Céline Hudelot, Mohamed El Amine Seddik, and Mohamed Tamaazousti. Learning more universal representations for transfer-learning. *IEEE transactions on pattern analysis and machine intelligence*, 2019.
- [54] Mingxing Tan and Quoc V Le. Efficientnet: Rethinking model scaling for convolutional neural networks. *arXiv preprint arXiv:1905.11946*, 2019.
- [55] Antonio Torralba, Kevin P Murphy, and William T Freeman. Sharing visual features for multiclass and multiview object detection. *IEEE Transactions on Pattern Analysis & Machine Intelligence*, (5):854–869, 2007.
- [56] Eric Tzeng, Judy Hoffman, Trevor Darrell, and Kate Saenko. Simultaneous deep transfer across domains and tasks. In *Proceedings of the IEEE International Conference on Computer Vision*, pages 4068–4076, 2015.
- [57] Vladimir Vapnik. *The nature of statistical learning theory*. Springer science & business media, 2013.
- [58] Oriol Vinyals, Charles Blundell, Timothy Lillicrap, Daan Wierstra, et al. Matching networks for one shot learning. In *Advances in neural information processing systems*, pages 3630–3638, 2016.
- [59] Qian Wang, Penghui Bu, and Toby P Breckon. Unifying unsupervised domain adaptation and zero-shot visual recognition. *arXiv preprint arXiv:1903.10601*, 2019.
- [60] Qian Wang and Ke Chen. Alternative semantic representations for zero-shot human action recognition. In *Joint European Conference on Machine Learning and Knowledge Discovery in Databases*, pages 87–102. Springer, 2017.
- [61] Wei Wang, Vincent W Zheng, Han Yu, and Chunyan Miao. A survey of zero-shot learning: Settings, methods, and applications. *ACM Transactions on Intelligent Systems and Technology (TIST)*, 10(2):13, 2019.
- [62] Wenlin Wang, Yunchen Pu, Vinay Kumar Verma, Kai Fan, Yizhe Zhang, Changyou Chen, Piyush Rai, and Lawrence Carin. Zero-shot learning via class-conditioned deep generative models. In *Thirty-Second AAAI Conference on Artificial Intelligence*, 2018.
- [63] Lior Wolf and Ian Martin. Robust boosting for learning from few examples. In *2005 IEEE Computer Society Conference on Computer Vision and Pattern Recognition (CVPR'05)*, volume 1, pages 359–364. IEEE, 2005.
- [64] Yongqin Xian, Zeynep Akata, Gaurav Sharma, Quynh Nguyen, Matthias Hein, and Bernt Schiele. Latent embeddings for zero-shot classification. In *Proceedings of the IEEE Conference on Computer Vision and Pattern Recognition*, pages 69–77, 2016.
- [65] Yongqin Xian, Bernt Schiele, and Zeynep Akata. Zero-shot learning - the good, the bad and the ugly. In *The IEEE Conference on Computer Vision and Pattern Recognition (CVPR)*, July 2017.
- [66] Xiaofeng Xu, Ivor W Tsang, and Chuancai Liu. Complementary attributes: A new clue to zero-shot learning. *IEEE transactions on cybernetics*, 2019.
- [67] Yunlong Yu, Zhongfei Zhang, and Jungong Han. Meta-transfer networks for zero-shot learning. *arXiv preprint arXiv:1909.03360*, 2019.
- [68] Sergey Zagoruyko and Nikos Komodakis. Wide residual networks. *arXiv preprint arXiv:1605.07146*, 2016.
- [69] Li Zhang, Tao Xiang, and Shaogang Gong. Learning a deep embedding model for zero-shot learning. In *Proceedings of the IEEE Conference on Computer Vision and Pattern Recognition*, pages 2021–2030, 2017.
- [70] Xiangyu Zhang, Xinyu Zhou, Mengxiao Lin, and Jian Sun. Shufflenet: An extremely efficient convolutional neural network for mobile devices. In *Proceedings of the IEEE Conference on Computer Vision and Pattern Recognition*, pages 6848–6856, 2018.
- [71] Bolei Zhou, Aditya Khosla, Agata Lapedriza, Aude Oliva, and Antonio Torralba. Learning deep features for discriminative localization. In *Proceedings of the IEEE conference on computer vision and pattern recognition*, pages 2921–2929, 2016.
- [72] Yi Zhu, Yang Long, Yu Guan, Shawn Newsam, and Ling Shao. Towards universal representation for unseen action recognition. In *Proceedings of the IEEE Conference on Computer Vision and Pattern Recognition*, pages 9436–9445, 2018.
- [73] Barret Zoph, Vijay Vasudevan, Jonathon Shlens, and Quoc V Le. Learning transferable architectures for scalable image recognition. In *Proceedings of the IEEE conference on computer vision and pattern recognition*, pages 8697–8710, 2018.
- [74] Pretrained deep neural networks - matlab & simulink - mathworks india. <https://in.mathworks.com/help/deeplearning/ug/pretrained-convolutional-neural-networks.html>. (Accessed on 05/13/2019).
- [75] Pretrained inception-v3 convolutional neural network - matlab inceptionv3 - mathworks india. <https://in.mathworks.com/help/deeplearning/ref/inceptionv3.html>. (Accessed on 05/13/2019).